Supporting Information

A Sulfone-functionalized Molecular Triangle as A Strong Anion Receptor Driven by Anion-π Interactions

Yifan Ma,[1] Zi-Hang Song,[1] Si-Dan Guo,[1] Han Han,[2] Kang Cai[1]*

[1]College of Chemistry, State Key Laboratory of Elemento-Organic Chemistry, Frontiers Science Center for New Organic Matter, Nankai University, Tianjin 300071, China

E-mail: kangcai@nankai.edu.cn

[2] Department of Chemistry, The University of Hong Kong, Hong Kong SAR 999077, China

Table of Contents

Section A. General Methods

All reagents were purchased from commercial suppliers and used without further purification. Thin-layer chromatography (TLC) was performed on silica gel HSGF254. UV-Vis Spectra were recorded in a quartz cell (light path 10 mm) on a Cary 100 UV-Vis spectrophotometer equipped with a Cary dual cell Peltier accessory. Nuclear magnetic resonance (NMR) spectra were recorded on Agilent DD2 500 and on Bruker Avance III 400 spectrometers, with working frequencies of 400 MHz for ^{1}H, as well as 100 MHz for ^{13}C nuclei, respectively. Chemical shifts are reported in ppm relative to the signals corresponding to the residual non-deuterated solvents ($CDCl_3$: δ_H = 7.26 ppm and δ_C = 77.0 ppm). High-resolution electrospray ionization-mass spectra (HR-ESI-MS) were recorded on a Bruker Apex IV Fourier transformation mass spectrometer. Fluorescence measurements were recorded in a conventional quartz cell (light path 10 mm) on a Cary Eclipse equipped with a Cary single-cell Peltier accessory.

Section B. Synthetic Protocols

Scheme S1. Synthesis of **(−)-PMDI-SO$_2$Et-Δ**.

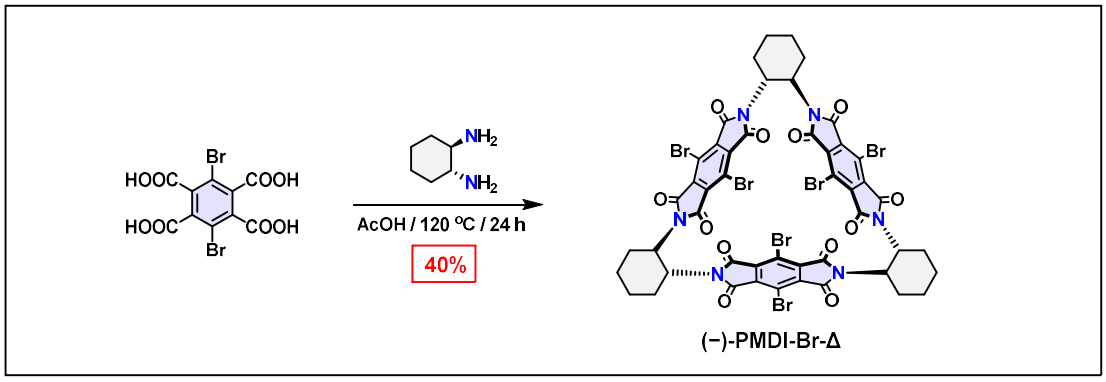

(−)-PMDI-Br-Δ:**(−)-PMDI-Br-Δ** was prepared using an improved protocol based on the method reported in the literature.[1] 3,6-Dibromobenzene-1,2,4,5-

tetracarboxylic acid (1.00 g, 2.42 mmol) was dissolved in 200 mL of AcOH. Over the course of one hour, (*RR*)–1,2-cyclohexanediamine (0.276 g, 2.42 mmol) was gradually added, ensuring complete dissolution with each successive addition. The reaction mixture was then heated up to reflux at 120 °C for 24 h. After completion, the reaction mixture was cooled and concentrated under reduced pressure to a final volume of approximately 50 mL. The resulting precipitate was filtered off, affording **(−)-PMDI-Br-**Δ as a white powder with an yield of 40%. **^{1}H NMR** (400 MHz, $CDCl_3$, ppm): δ_H = 5.25 – 5.13 (s, 6H), 2.18 – 1.82 (s, 18H), 1.59 – 1.50 (m, 6H). **^{13}C NMR** (100 MHz, $CDCl_3$, ppm): δ = 162.88, 162.22 135.52, 135.43, 114.22, 51.32, 30.64, 24.95.

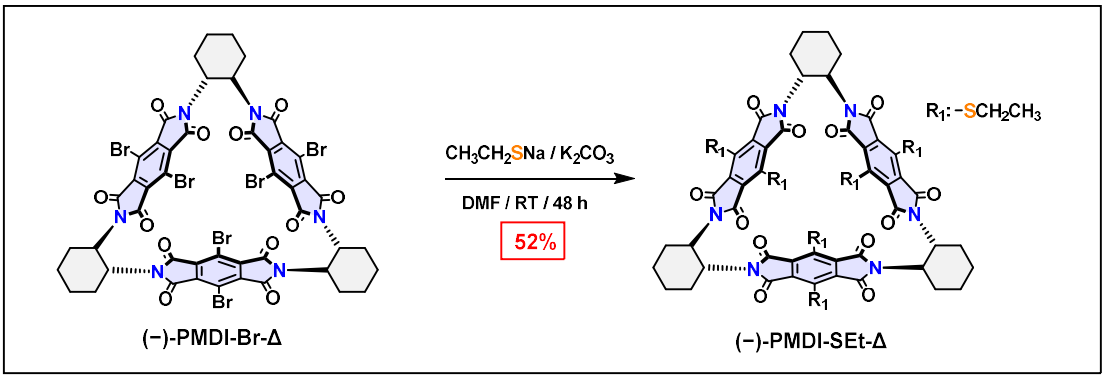

(−)-PMDI-SEt-Δ**:** A Schlenk tube containing **(−)-PMDI-Br-**Δ (200 mg, 0.147 mmol) and K_2CO_3 (160 mg, 1.16 mmol) was evacuated and backfilled with nitrogen. Degassed DMF (30 mL) and sodium ethanethiolate (75 mg, 0.892 mmol) were then added, and the mixture was stirred at room temperature for 48 h. Upon completion, the mixture was poured into cold water and extracted with CH_2Cl_2. The combined organic layers were dried over anhydrous Na_2SO_4 and concentrated under reduced pressure. The crude product was purified by silica gel column chromatography (CH_2Cl_2 / EtOAc = 40 / 1) to afford **(−)-PMDI-SEt-**Δ as an orange red solid (96 mg, 52% yield). **^{1}H NMR** (400 MHz, $CDCl_3$, ppm): δ_H = 5.18 – 5.10 (m, 6H), 3.21 – 2.90 (m, 12H), 2.19 – 1.92 (m, 12H), 1.91 – 1.82 (m, 6H), 1.58 – 1.46 (m, 6H) , 1.03 – 0.97 (m, 18H). **^{13}C NMR** (100 MHz, $CDCl_3$, ppm): δ =164.35, 163.54, 136.23, 135.91, 134.50, 51.32, 31.25,

30.73, 25.10, 14.42. **HR-ESI MS**: found m/z = 1266.3040, calculated m/z for $C_{60}H_{60}N_6O_{12}S_6$ $[M+NH_4]^+$ =1266.2932.

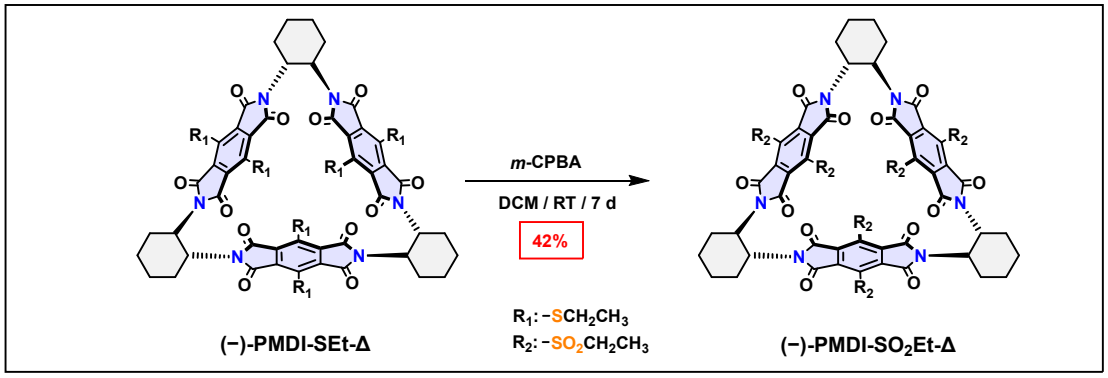

(−)-PMDI-SO_2Et-Δ： **(−)-PMDI-SEt-**Δ (200 mg, 0.16 mmol) was dissolved in DCM (30.0 mL) and cooled to 0 °C. *m*-CPBA (335 mg, 1.94 mmol) was added in portions over the course of 1 h. The mixture was then allowed to stir at room temperature for 7 days. After completion, the mixture was poured into cold water and extracted with CH_2Cl_2. The combined organic layers were dried over anhydrous Na_2SO_4 and concentrated under reduced pressure. The crude product was purified by silica gel column chromatography (CH_2Cl_2 / MeOH = 20 / 1) to afford **(−)-PMDI-SO_2Et-**Δ as a white solid (98 mg, 42% yield). **^{1}H NMR** (400 MHz, $CDCl_3$, ppm): δ_H = 5.12 – 4.96 (m, 6H), 3.80 – 3.64 (m, 12H), 2.18 – 2.01 (m, 12H), 1.96 – 1.85 (m, 6H), 1.56 – 1.41 (m, 24H) . **^{13}C NMR** (100 MHz, $CDCl_3$, ppm): δ_H = 161.27, 160.62, 140.83, 138.51, 137.83, 52.77, 50.00, 30.22, 24.87, 6.03. **HR-ESI MS**: found m/z = 1458.2312, calculated m/z for $C_{60}H_{60}N_6O_{24}S_6$ $[M+NH_4]^+$ = 1458.2322.

Section C. NMR Spectroscopy

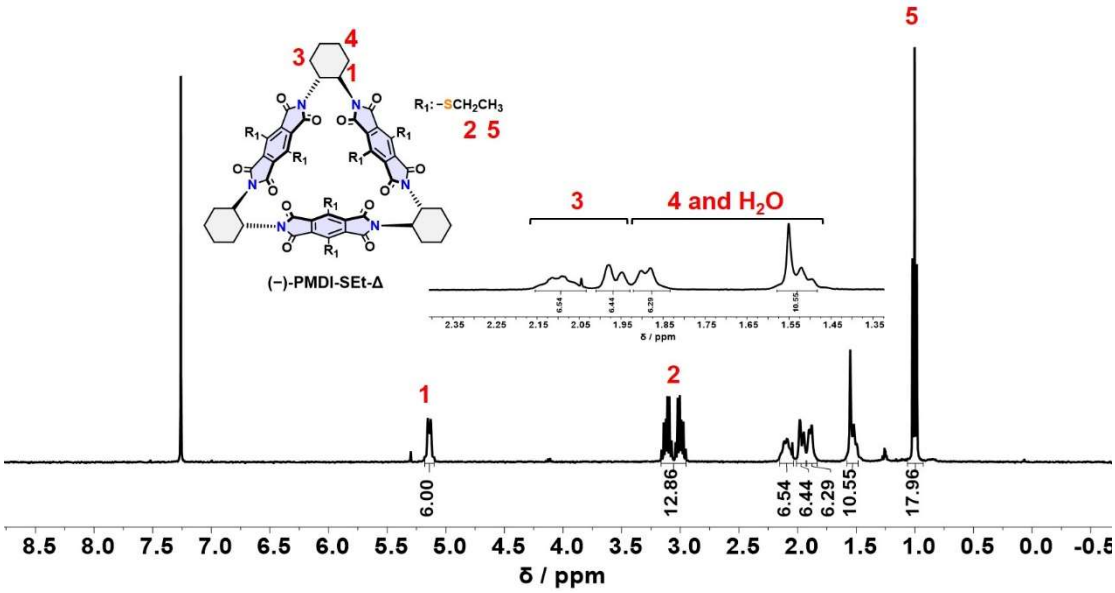

Figure S1 ^{1}H NMR Spectrum (400 MHz / $CDCl_3$ / 298 K) of **(−)-PMDI-SEt-Δ**

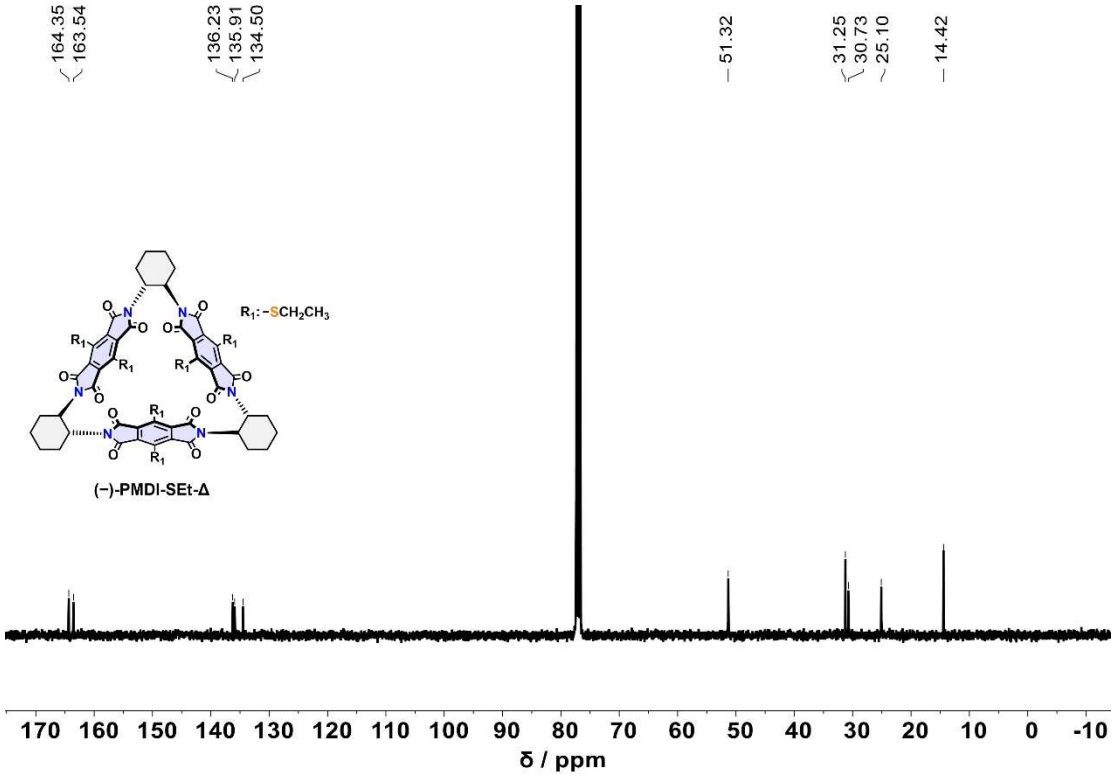

Figure S2 ^{13}C NMR Spectrum (100 MHz / $CDCl_3$ / 298 K) of **(−)-PMDI-SEt-Δ**

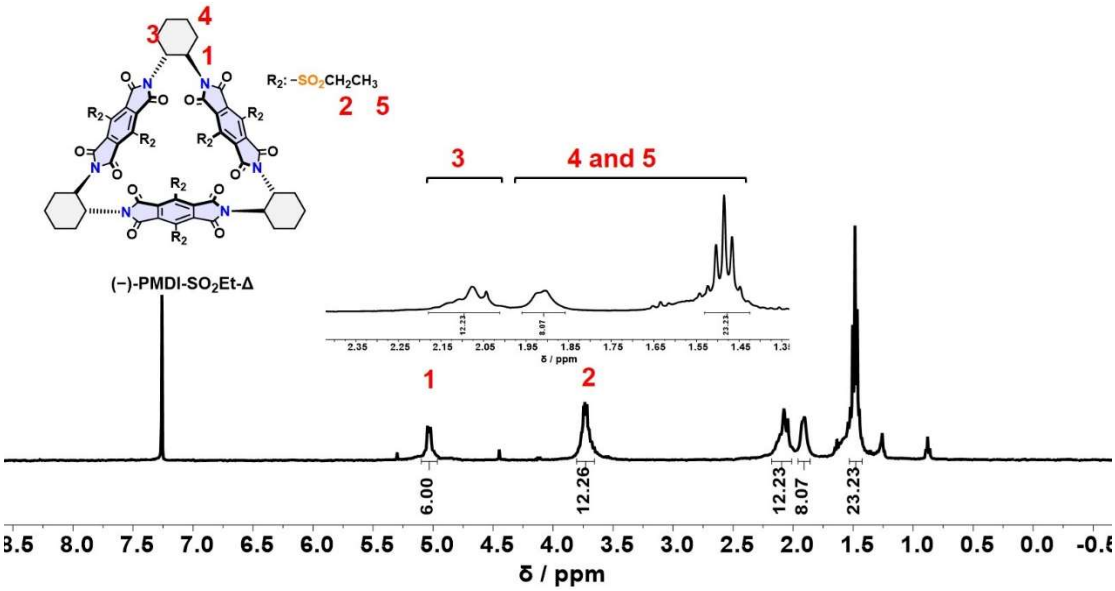

Figure S3 ^{1}H NMR Spectrum (400 MHz / $CDCl_3$ / 298 K) of **(−)-PMDI-SO_2Et-Δ**

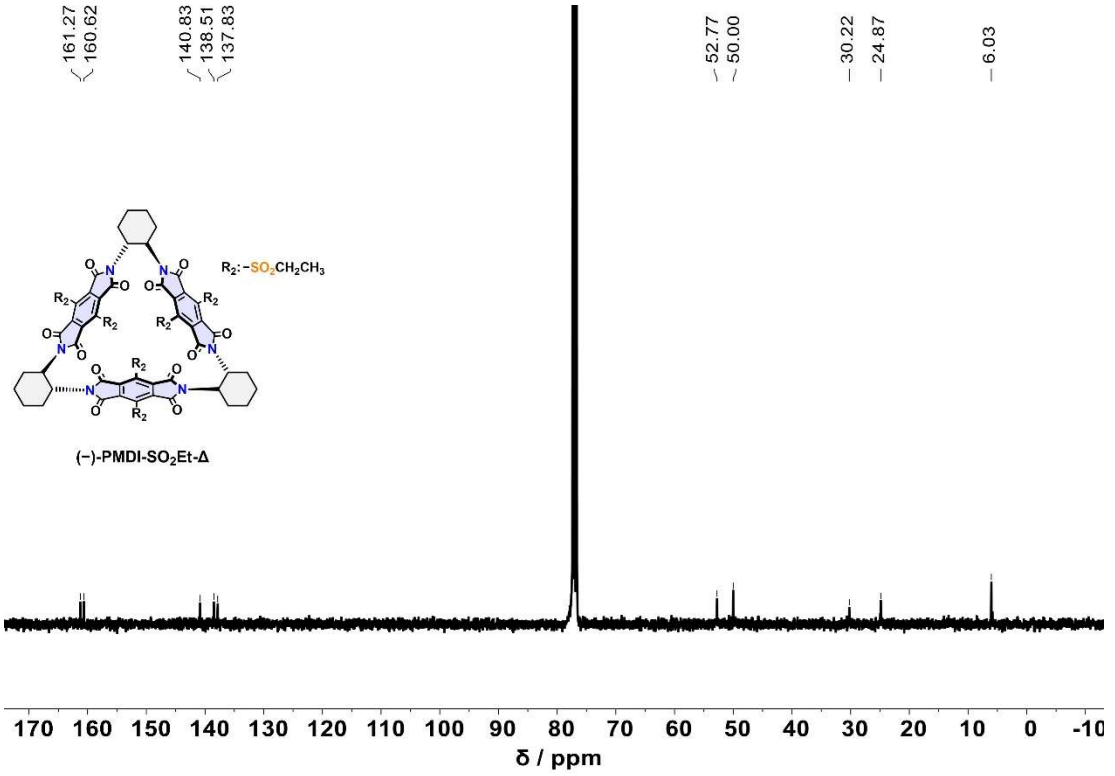

FigureS4 ^{13}C NMR Spectrum (100 MHz / $CDCl_3$ / 298 K) of **(−)-PMDI-SO_2Et-Δ**

Section D. UV–Vis Titrations

UV-Vis titration experiments were conducted to monitor the absorbance changes of **(−)-PMDI-SO_2Et-Δ** and **(−)-PMDI-Δ** upon the incremental addition of various equivalents of guests. The absorbance intensity at a selected

wavelength was plotted against guest concentration and fitted to a 1:1 binding model based on a nonlinear least-squares fitting equation[2] using Origin Lab 9.1 software, affording the binding constant (K_a). As suggested by a reviewer, we also re-analyzed all the data using BindFit (http://supramolecular.org/), and the results were in good agreement with those obtained from Origin. The BindFit fitting results have been included as hyperlinks in Section F for reference.

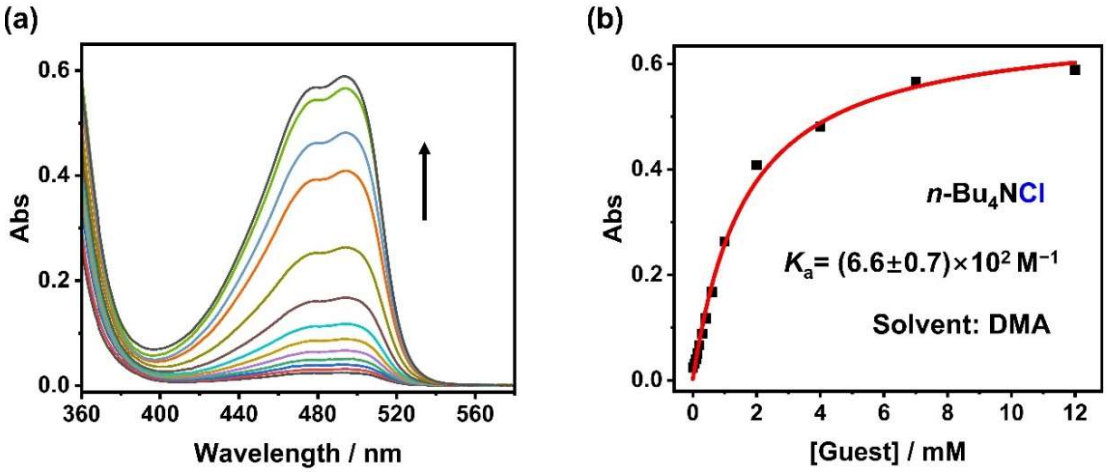

Figure S5 (a) UV–Vis titration spectra of **(−)-PMDI-SO_2Et-Δ** (0.20 mM in DMA) upon the addition of *n*-Bu_4NCl (up to 12.0 mM). (b) The corresponding titration curve at λ_{abs} = 492 nm, fitted according to a 1:1 binding model.

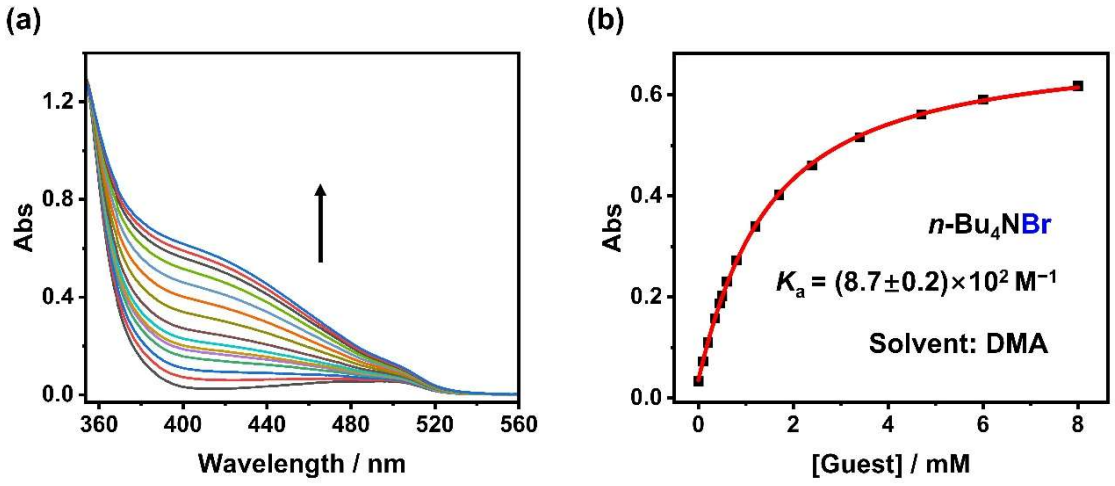

Figure S6 (a) UV–Vis titration spectra of **(−)-PMDI-SO_2Et-Δ** (0.50 mM in DMA) upon the addition of *n*-Bu_4NBr (up to 8.0 mM). (b) The corresponding titration curve at λ_{abs} = 400 nm, fitted according to a 1:1 binding model.

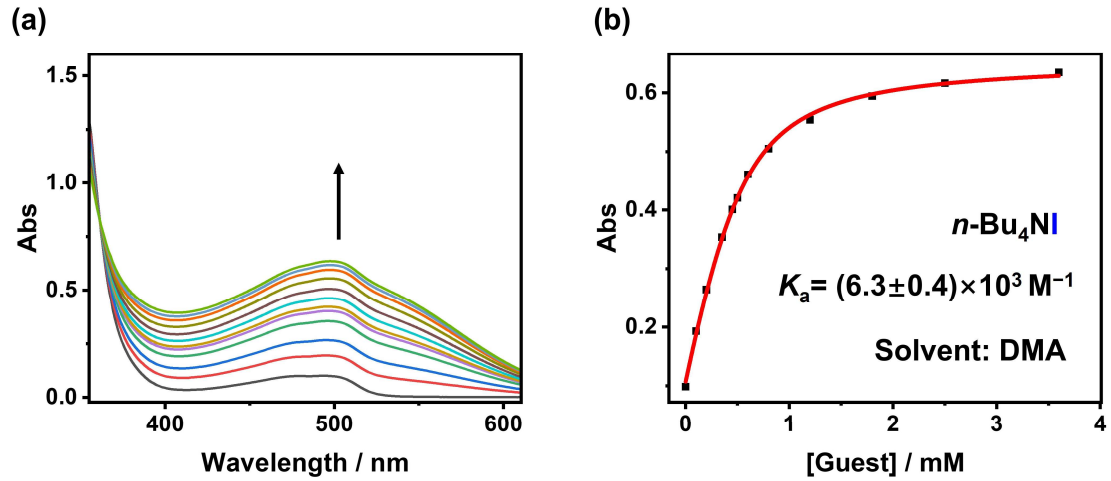

Figure S7 (a) UV–Vis titration spectra of **(−)-PMDI-SO$_2$Et-Δ** (0.50 mM in DMA) upon the addition of *n*-Bu$_4$NI (up to 3.6 mM). (b) The corresponding titration curve at λ_{abs} = 500 nm, fitted according to a 1:1 binding model.

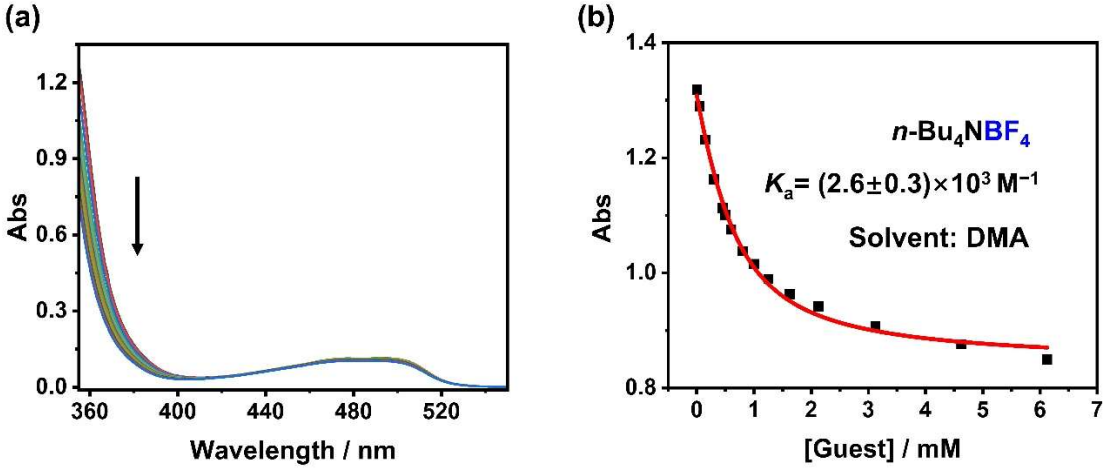

Figure S8 (a) UV–Vis titration of **(−)-PMDI-SO$_2$Et-Δ** (0.50 mM in DMA) upon the addition of *n*-Bu$_4$NBF$_4$ (up to 6.125 mM). (b) The corresponding titration curve at λ_{abs} = 363 nm, fitted according to a 1:1 binding model.

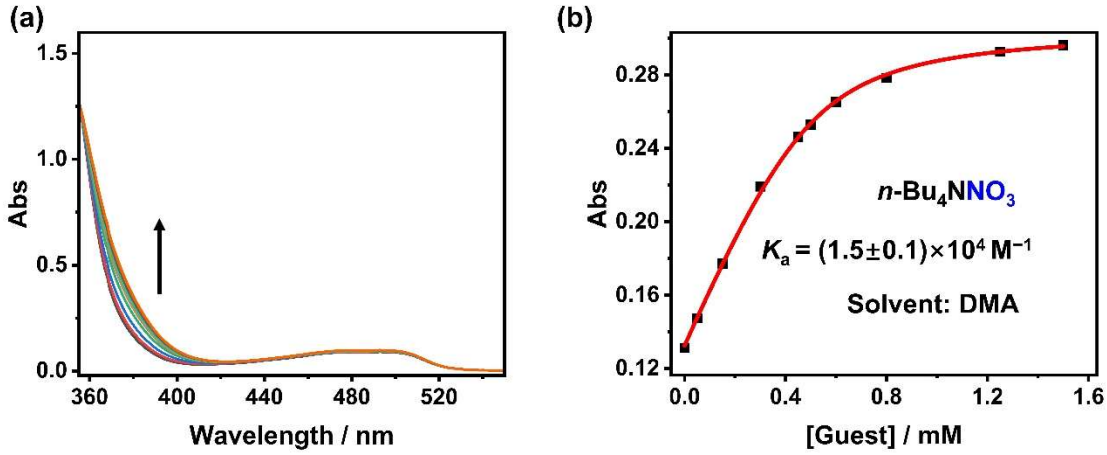

Figure S9 (a) UV–Vis titration spectra of **(−)-PMDI-SO$_2$Et-Δ** (0.50 mM in DMA) upon the addition of *n*-Bu$_4$NNO$_3$ (up to 1.5 mM). (b) The corresponding titration curve at λ_{abs} = 383 nm, fitted according to a 1:1 binding model.

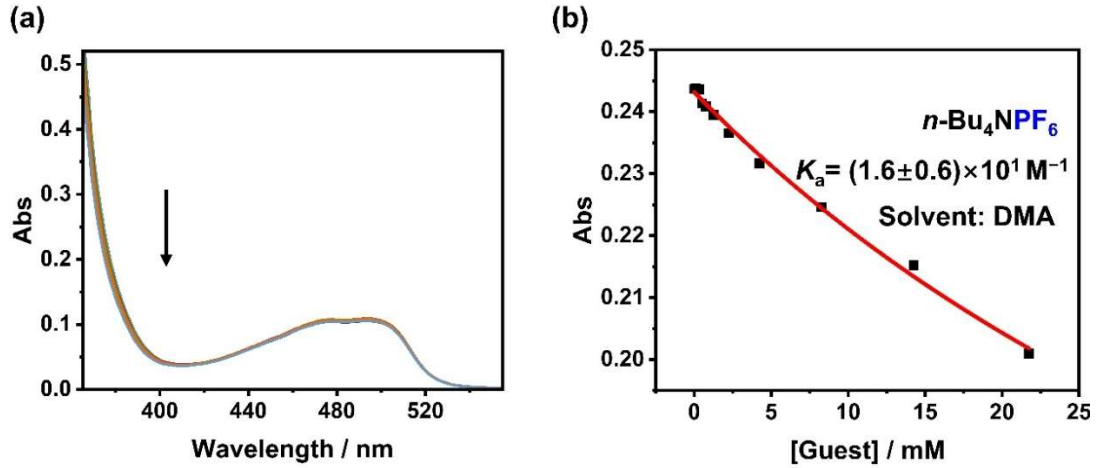

Figure S10 (a) UV–Vis titration of **(−)-PMDI-SO$_2$Et-Δ** (0.50 mM in DMA) upon the addition of *n*-Bu$_4$NPF$_6$ (up to 21.75 mM). (b) The corresponding titration curve at λ_{abs} = 375 nm, fitted according to a 1:1 binding model.

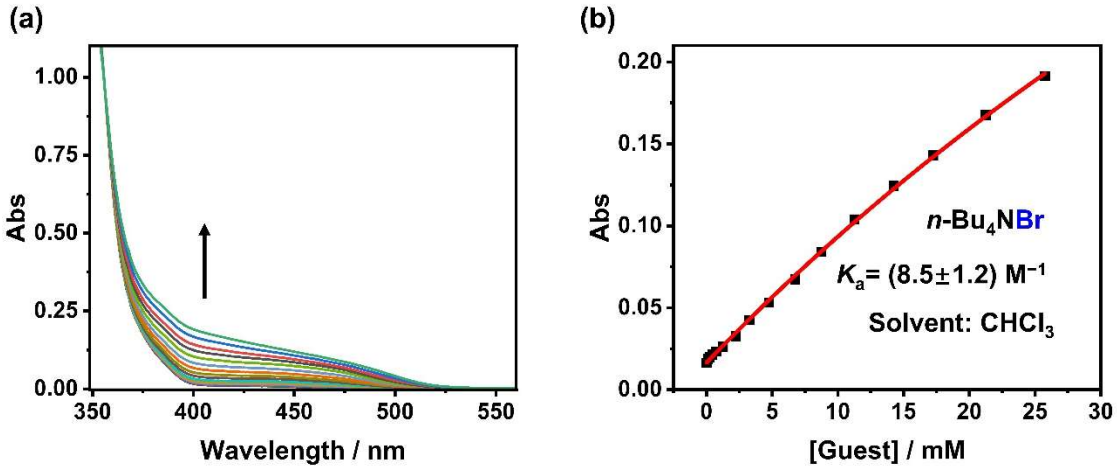

Figure S11 (a) UV–Vis titration spectra of **(−)-PMDI-SO$_2$Et-Δ** (0.50 mM in $CHCl_3$) upon the addition of *n*-Bu_4NBr (up to 25.75 mM). (b) The corresponding titration curve at λ_{abs} = 400 nm, fitted according to a 1:1 binding model.

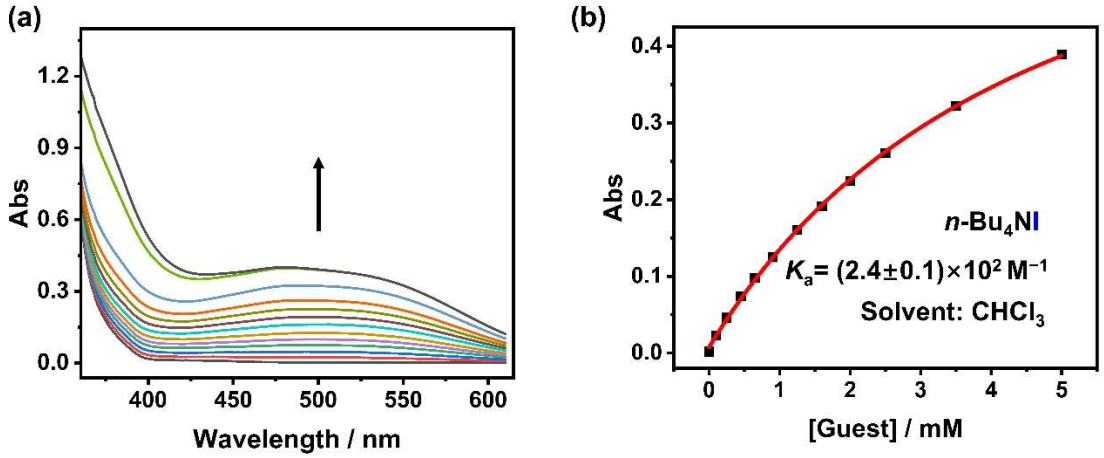

Figure S12 (a) UV–Vis titration spectra of **(−)-PMDI-SO$_2$Et-Δ** (0.50 mM in $CHCl_3$) upon the addition of *n*-Bu_4NI (up to 5.0 mM). (b) The corresponding titration curve at λ_{abs} = 500 nm, fitted according to a 1:1 binding model.

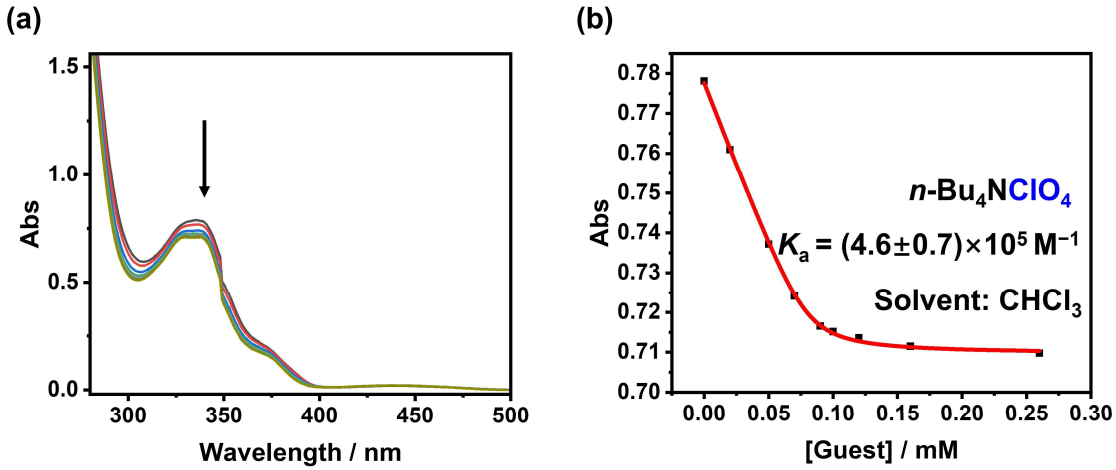

Figure S13 (a) UV–Vis titration spectra of **(−)-PMDI-SO$_2$Et-Δ** (0.08 mM in $CHCl_3$) upon the addition of *n*-Bu_4NClO_4 (up to 0.26 mM). (b) The corresponding titration curve at λ_{abs} = 330 nm, fitted according to a 1:1 binding model.

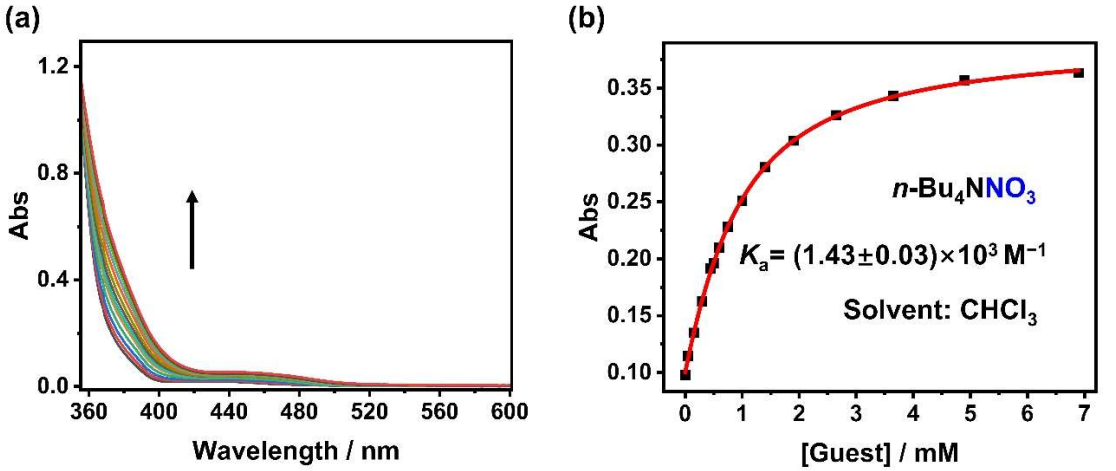

Figure S14 (a) UV–Vis titration spectra of **(−)-PMDI-SO$_2$Et-Δ** (0.50 mM in $CHCl_3$) upon the addition of *n*-Bu_4NNO_3 (up to 6.9 mM). (b) The corresponding titration curve at λ_{abs} = 367 nm, fitted according to a 1:1 binding model.

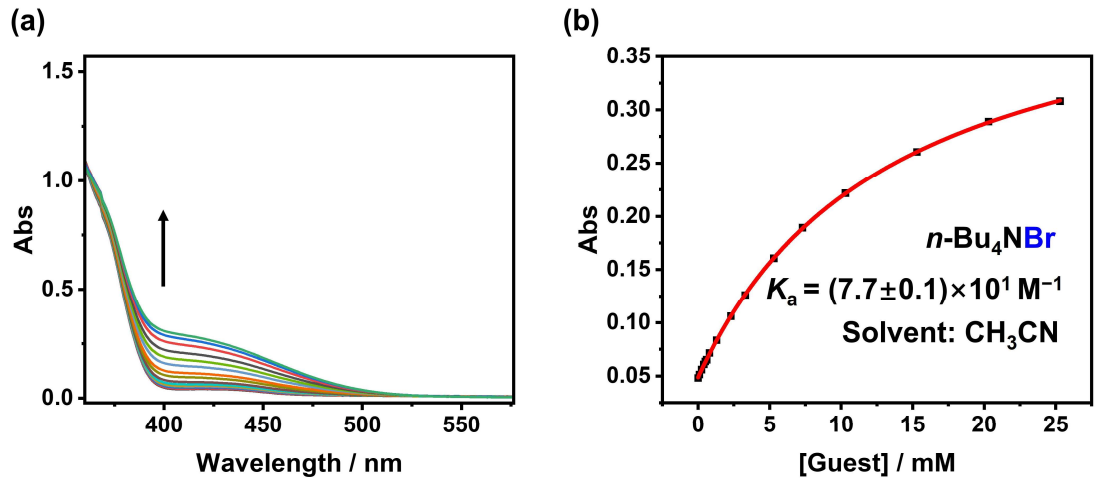

Figure S15 (a) UV–Vis titration spectra of **(−)-PMDI-SO_2Et-Δ** (0.50 mM in CH_3CN) upon the addition of *n*-Bu_4NBr (up to 25.3 mM). (b) The corresponding titration curve at λ_{abs} = 400 nm, fitted according to a 1:1 binding model.

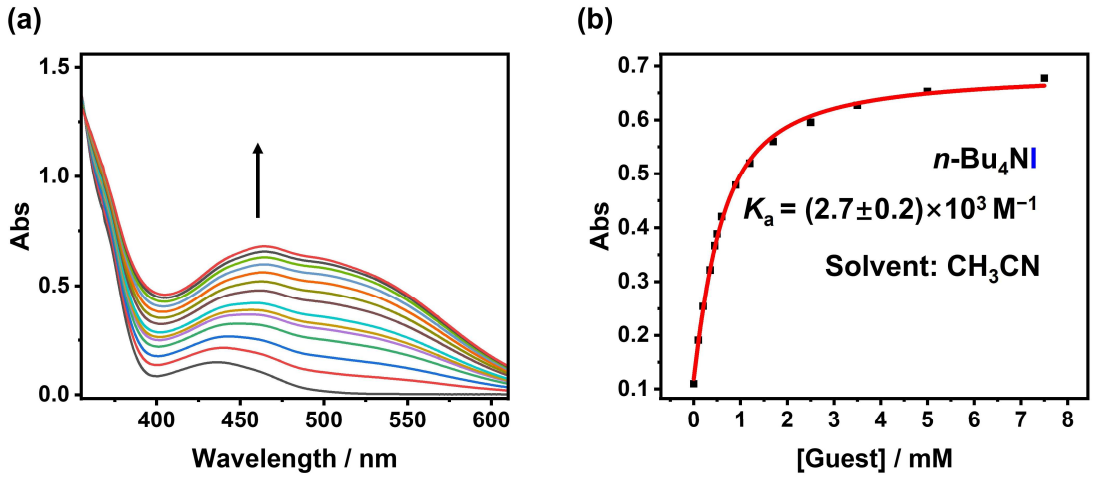

Figure S16 (a) UV–Vis titration spectra of **(−)-PMDI-SO_2Et-Δ** (0.40 mM in CH_3CN) upon the addition of *n*-Bu_4NI (up to 7.5 mM). (b) The corresponding titration curve at λ_{abs} = 460 nm, fitted according to a 1:1 binding model.

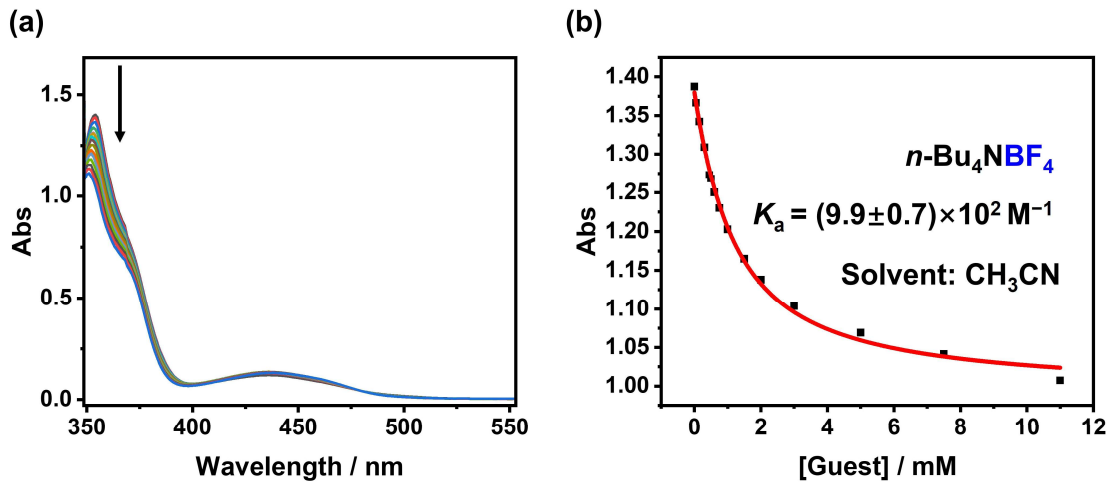

Figure S17 (a) UV–Vis titration spectra of **(−)-PMDI-SO$_2$Et-Δ** (0.40 mM in CH_3CN) upon the addition of *n*-Bu_4NBF_4 (up to 11.0 mM). (b) The corresponding titration curve at λ_{abs} = 355 nm, fitted according to a 1:1 binding model.

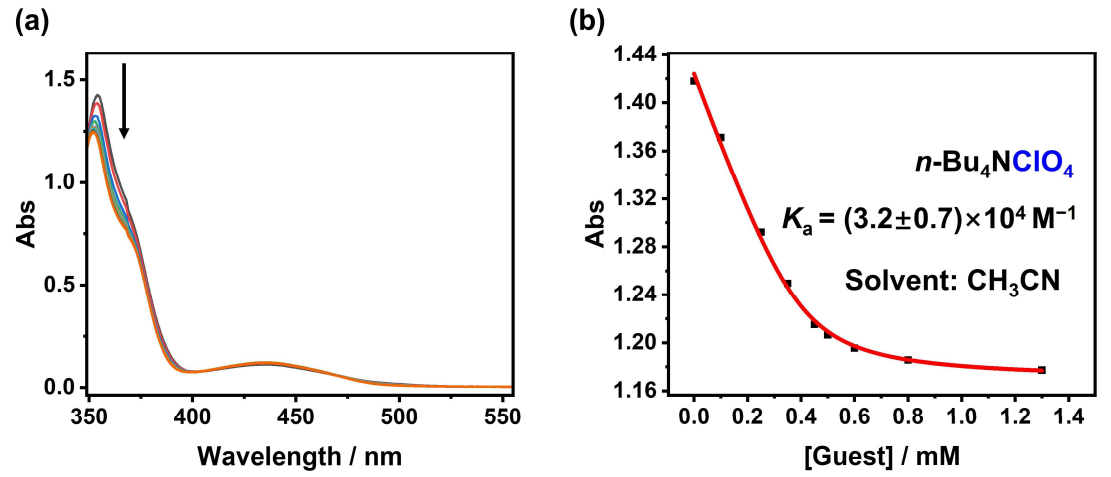

Figure S18 (a) UV–Vis titration spectra of **(−)-PMDI-SO$_2$Et-Δ** (0.40 mM in CH_3CN) upon the addition of *n*-Bu_4NClO_4 (up to 1.3 mM). (b) The corresponding titration curve at λ_{abs} = 355 nm, fitted according to a 1:1 binding model.

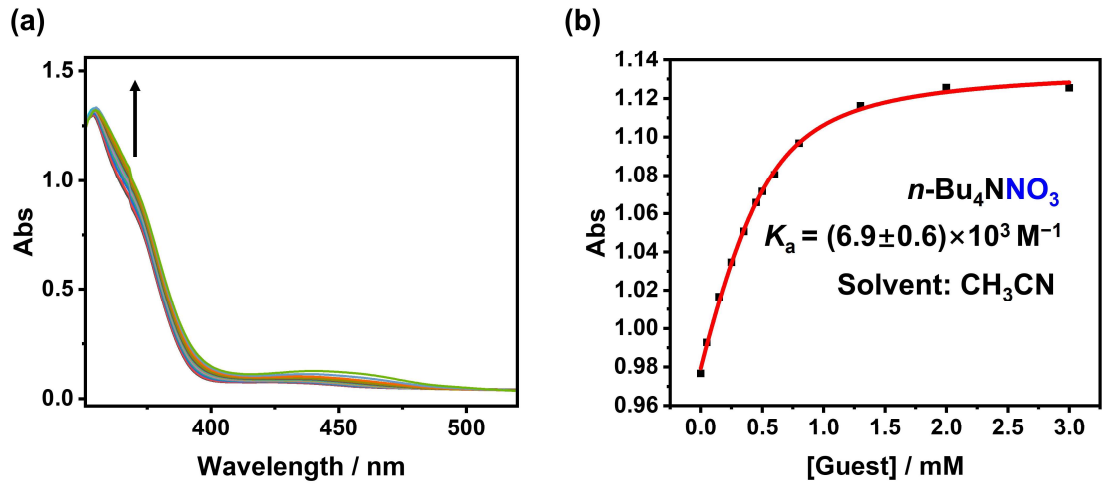

Figure S19 (a) UV–Vis titration spectra of **(−)-PMDI-SO_2Et-Δ** (0.50 mM in CH_3CN) upon the addition of *n*-Bu_4NNO_3 (up to 3.0 mM). (b) The corresponding titration curve at λ_{abs} = 365 nm, fitted according to a 1:1 binding model.

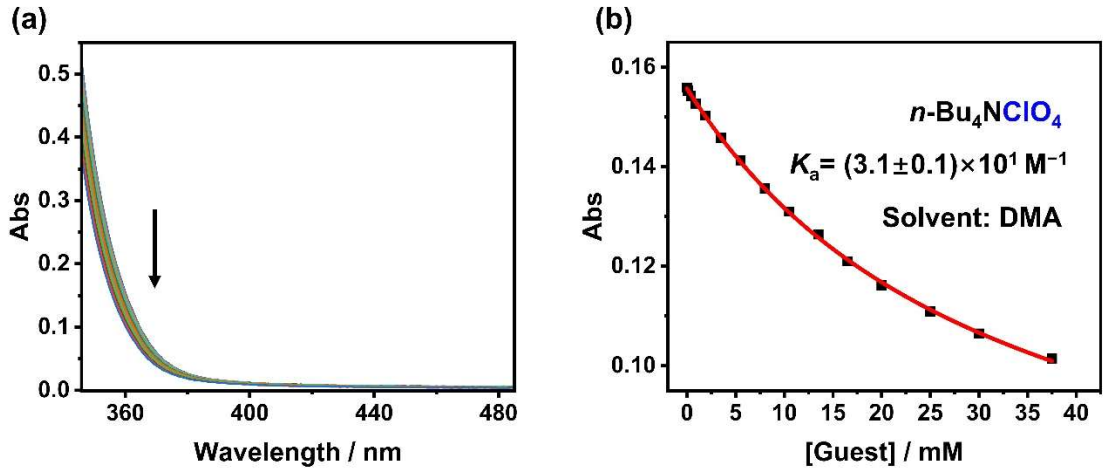

Figure S20 (a) UV–vis titration spectra of **(−)-PMDI-Δ** (0.50 mM in DMA) upon the addition of *n*-Bu_4NClO_4 (up to 37.5 mM). (b) The corresponding titration curve at λ_{abs} = 360 nm, fitted according to a 1:1 binding model.

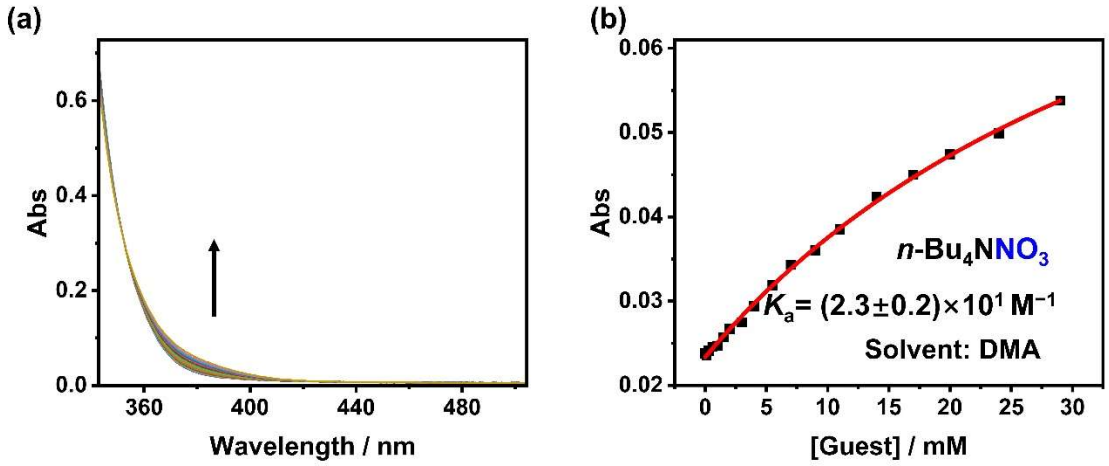

Figure S21 (a) UV–Vis titration spectra of **(−)-PMDI-Δ** (0.50 mM in DMA) upon the addition of *n*-Bu4NNO3 (up to 29.0 mM). (b) The corresponding titration curve at λ_{abs} = 382 nm, fitted according to a 1:1 binding model.

Section E. ^{1}H NMR Titrations

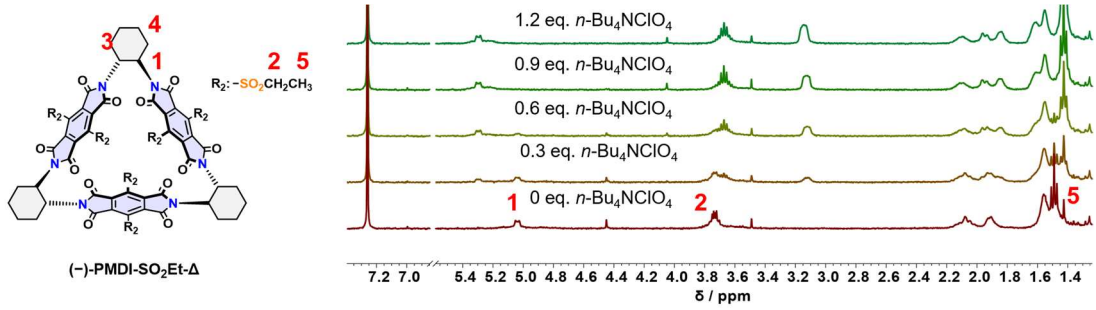

Figure S22 ^{1}H NMR titration spectra of **(−)-PMDI-SO2Et-Δ** (1.0 mM in $CDCl_3$) upon addition of *n*-Bu4NClO4 (up to 1.2 mM).

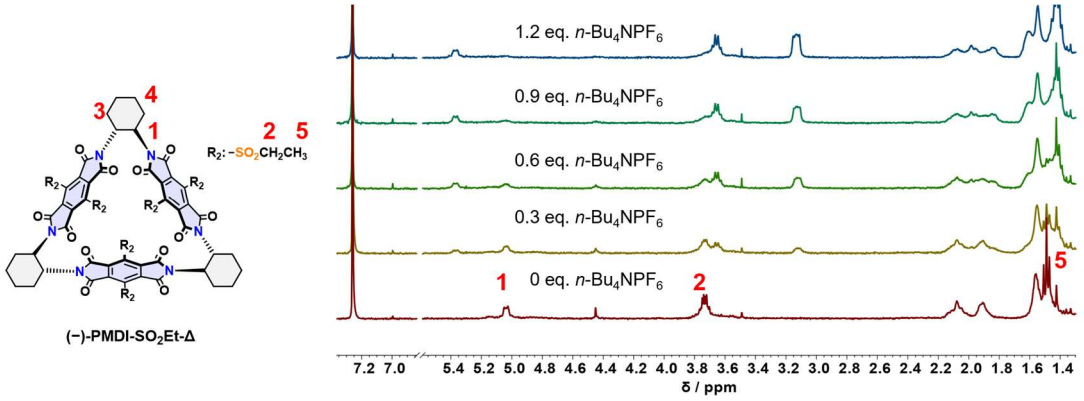

Figure S23 ^{1}H NMR titration spectra of **(−)-PMDI-SO2Et-Δ** (1.0 mM in $CDCl_3$) upon addition of *n*-Bu4NPF6 (up to 1.2 mM).

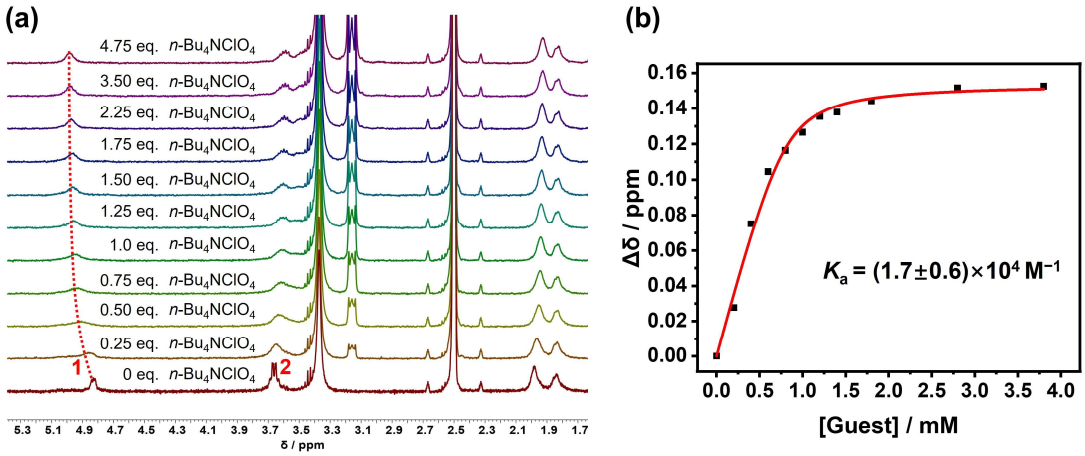

Figure S24 (a) ^{1}H NMR titration spectra of **(−)-PMDI-SO$_2$Et-Δ** (0.80 mM in DMSO-d$_6$) upon addition of *n*-Bu$_4$NClO$_4$ (up to 3.8 mM). (b) The corresponding titration curve at chemical shift of the protons **1** of **(−)-PMDI-SO$_2$Et-Δ** , fitted according to a 1:1 binding model.

Section F. Bindfit URL List of Titrations

Bindfit URL List for (−)-PMDI-SO$_2$Et-Δ Titrations in DMA

TBA$^+$Cl$^-$
http://app.supramolecular.org/bindfit/view/55135d4a-9bf1-4ee7-a565-f5b73e16bf30
TBA$^+$Br$^-$
http://app.supramolecular.org/bindfit/view/f94e4994-7473-4e21-86f7-89d47359fd18
TBA$^+$I$^-$
http://app.supramolecular.org/bindfit/view/e38bfeb9-cdbd-46a0-9874-0e86c33acbb0
TBA$^+$BF$_4^-$
http://app.supramolecular.org/bindfit/view/5378c874-ab7d-4a7b-93c1-0bc8aeff9884
TBA$^+$NO$_3^-$
http://app.supramolecular.org/bindfit/view/c13cb480-47ff-443d-8da0-a90c4e726781
TBA$^+$PF$_6^-$
http://app.supramolecular.org/bindfit/view/585a762d-db19-47da-94a0-93926adffcaf
TBA$^+$ClO$_4^-$
http://app.supramolecular.org/bindfit/view/d73b38c2-e8ff-4602-a27d-7356d6b4f535

Bindfit URL List for (−)-PMDI-SO$_2$Et-Δ Titrations in CHCl$_3$

TBA$^+$Br$^-$
http://app.supramolecular.org/bindfit/view/6e14eb66-495c-4c49-99d9-5f194d972e38
TBA$^+$I$^-$
http://app.supramolecular.org/bindfit/view/7740e202-56f7-4d91-8162-b7789ce600a0
TBA$^+$NO$_3^-$
http://app.supramolecular.org/bindfit/view/6a605b8d-25e8-4d38-9cb2-ed9e7edb67f7

$TBA^+ClO_4^-$
http://app.supramolecular.org/bindfit/view/2031e58a-7148-490e-ad71-400480949d7c

Bindfit URL List for (−)-PMDI-SO_2Et-Δ Titrations in CH_3CN

TBA^+Br^-
http://app.supramolecular.org/bindfit/view/d276d271-4f60-433f-bf56-f0aa1efbca81
TBA^+I^-
http://app.supramolecular.org/bindfit/view/8a48f038-70dc-4292-9294-4105b6d4e0c2
$TBA^+BF_4^-$
http://app.supramolecular.org/bindfit/view/664c4a48-c68c-4940-abfa-36f12cda7b53
$TBA^+NO_3^-$
http://app.supramolecular.org/bindfit/view/ce4627aa-5f25-48cf-b463-9d5b637579c2
$TBA^+ClO_4^-$
http://app.supramolecular.org/bindfit/view/070aab5e-651a-4e37-ae52-2de05db16ba4

Bindfit URL List for (−)-PMDI-Δ Titrations in DMA

$TBA^+NO_3^-$
http://app.supramolecular.org/bindfit/view/0aa07673-3b14-46aa-ad71-8afeb655664b
$TBA^+ClO_4^-$
http://app.supramolecular.org/bindfit/view/8a5ea380-1b6a-4eed-8974-41335c6f81af

Section G. Crystallographic Characterization

The single crystals of **(−)-PMDI-SO_2Et-Δ** were obtained by evaporating ethanol into a $C_2H_4Cl_2$ solution of **(−)-PMDI-SO_2Et-Δ** slowly at 25 ℃. The single crystals of **(−)-PMDI-SO_2Et-Δ@***n*-Bu_4NClO_4 complex were obtained by evaporating isopropyl ether into the DMA solution of **(−)-PMDI-SO_2Et-Δ@***n*-Bu_4NClO_4 slowly at 25 ℃.

Table S1 Summary of x-ray crystallographic data and structure refinement for **(−)-PMDI-SO_2Et-Δ** and **(−)-PMDI-SO_2Et-Δ@***n*-Bu_4NClO_4

	(−)-PMDI-SO_2Et-Δ	**(−)-PMDI-SO_2Et-Δ@** *n*-Bu_4NClO_4
CCDC number	2380130	2380119
Empirical formula	$C_{60}H_{60}N_6O_{24}S_6 \cdot C_2H_4Cl_2 \cdot H_2O$	$C_{76}H_{96}ClN_7O_{28}S_6$
Formula weight	1558.46	1783.40
Temperature/K	170.00	170.00
Crystal system	Monoclinic	Monoclinic
Space group	$P2_1$	$P2$
a/Å	14.5385(8)	15.2633(5)

b/Å	20.3950(10)	16.5145(6)
c/Å	17.6470(10)	17.4282(6)
α/°	90	90
β/°	103.576(3)	90.100(5)
γ/°	90	90
Volume/Å^3	5086.4(5)	4393.0(3)
Z	2	2
ρ_{calcg}/cm^3	1.018	1.348
μ/mm^{-1}	1.461	1.571
F(000)	1620.0	1876.0
Crystal size/mm^3	0.17 × 0.17 × 0.05	0.17 × 0.17 × 0.056
Radiation	GaK_α (λ = 1.34139)	GaK_α (λ = 1.34139)
2Θ range for data collection/°	5.44 to 111.022	5.036 to 109.874
Index ranges	-16≤ *h* ≤16, -22≤ *k* ≤ 22, -19≤ *l* ≤ 19	-16≤ *h* ≤18, -20≤ *k* ≤19, -21≤*l* ≤21
Reflections collected	77165	40157
Independent reflections	19076 [R_{int} = 0.1257, R_{sigma} = 0.1148]	16291 [R_{int} = 0.0604, R_{sigma} = 0.0791]
Data/restraints/parameters	19076/102/920	16291/1005/1294
Goodness-of-fit on F^2	0.965	1.156
Final R indexes [*I*>=2σ (*I*)]	R_1 = 0.0784, wR_2 = 0.2144	R_1 = 0.1043, wR_2 = 0.2838
Final R indexes [all data]	R_1 = 0.1297, wR_2 = 0.2495	R_1 = 0.1425, wR_2 = 0.3174
Largest diff. peak/hole / eÅ^{-3}	0.35/-0.42	1.01/-0.66
Flack parameter	0.231(16)	0.101(12)

Table S2 Bond distances and angles of the hydrogen bonds

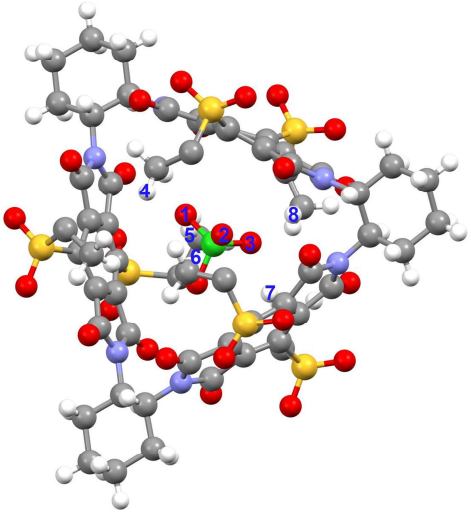

	H···O(Å)	C−H···O (°)
C−H4···O1	2.86	161.61
C−H5···O1	2.72	161.21
C−H4···O2	2.88	117.55
C−H6···O2	2.51	154.96
C−H7···O3	2.39	158.13
C−H8···O3	2.64	162.26

Section H. Theoretical Calculations

In this study, all Density Functional Theory (DFT) Calculations were conducted using the Gaussian 09 program.[3] Geometry optimization and frequency calculations were carry out at the B3LYP/6-31G(d)[4-6] level of theory. No constraints were imposed during the optimization, and the default convergence criteria of the Gaussian 09 program were employed. The optimized geometry exhibited no imaginary frequencies. Electrostatic potential (ESP) and independent gradient model (IGM) analyses were performed using the Multifunctional Wave-function Analyser (Multiwfn)[7] program and visualized using VMD software[8] (http://www.ks.uiuc.edu/Research/vmd/).

1) Electrostatic potential map

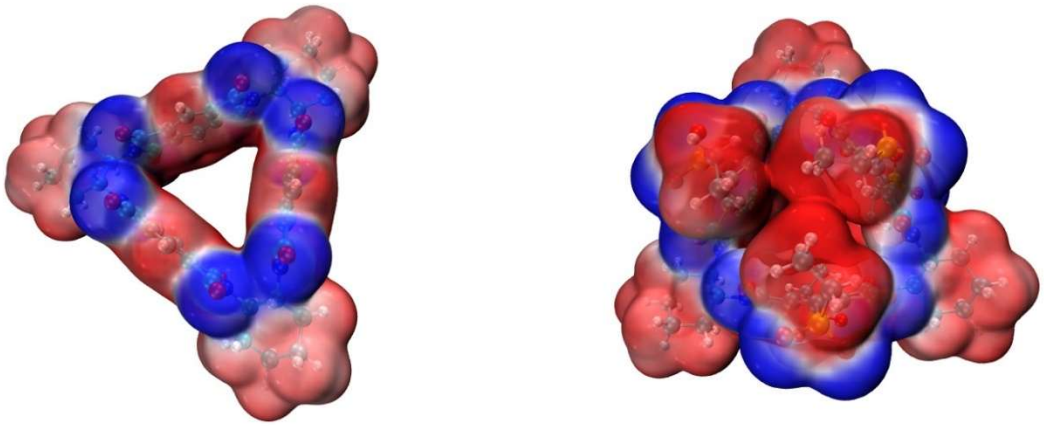

Figure S25. Top-down views of electrostatic potential (ESP) map of **(−)-PMDI-**Δ (left) and **(−)-PMDI-SO$_2$Et-**Δ (right).

2) Optimized geometry coordinates

(−)-PMDI-SO$_2$Et-Δ

S	-4.62447	2.89999	2.61455
S	-3.30748	2.51081	-3.50258
S	-0.50574	-4.81855	-3.13487
O	-5.86446	2.12102	2.62569
O	-4.6797	4.36015	2.48852

O	-5.16449	-0.42105	1.75471
O	-4.00462	-0.60848	-2.6664
O	-2.99745	3.92056	-3.74827
O	-4.66237	2.00522	-3.74675
O	-0.78699	4.45178	-2.1459
O	-1.80068	4.5872	2.31863
O	-3.10694	-3.04312	2.37738
O	-1.61362	-5.77233	-3.0253
O	0.83549	-5.29201	-3.4867
O	-3.42229	-3.67736	-2.14616
N	-4.87571	-0.75351	-0.52002
N	-1.15418	4.85898	0.10641
N	-3.63201	-3.41081	0.14853
C	-3.6726	2.35107	1.11313
C	-4.05178	1.25439	0.32938
C	-4.79123	-0.02358	0.67575
C	-4.21358	-0.12195	-1.57497
C	-3.72482	1.19452	-1.03372
C	-3.03164	2.2194	-1.68724
C	-2.12181	1.45419	-4.38294
H	-2.38931	0.43356	-4.09809
H	-2.40385	1.60661	-5.43113
C	-0.66219	1.81111	-4.12425
H	-0.37992	1.6219	-3.08346
H	-0.46345	2.86259	-4.34092
H	-0.02658	1.18795	-4.76281
C	-2.43355	3.16495	-0.8463
C	-1.38994	4.22957	-1.1202
C	-1.9023	4.2952	1.14778

C	-2.74384	3.21507	0.52058
C	-0.25818	6.00438	0.34519
H	-0.11343	6.00526	1.42692
C	-0.94675	7.31966	-0.07502
H	-1.12897	7.3014	-1.15773
H	-1.92379	7.3738	0.41797
C	-0.08926	8.53716	0.30001
H	-0.01658	8.60345	1.39463
H	-0.58592	9.45413	-0.03753
C	-5.58448	-2.03526	-0.68582
H	-5.37629	-2.32769	-1.71714
C	-5.07882	-3.15508	0.25906
H	-5.21947	-2.83196	1.29291
C	-2.78756	-3.41886	1.27443
C	-1.42684	-3.83303	0.76546
C	-1.50054	-3.88767	-0.63465
C	-0.37006	-4.0797	-1.43567
C	-0.98336	-3.46605	-4.24768
H	-1.16665	-3.99101	-5.19228
H	-1.9402	-3.09803	-3.86882
C	0.08832	-2.39047	-4.38848
H	1.04404	-2.81946	-4.6971
H	0.24716	-1.85319	-3.44773
H	-0.23638	-1.66473	-5.14206
C	-2.94319	-3.68179	-1.03141
C	-5.86543	-4.45945	0.01233
H	-5.64802	-4.82193	-1.00014
H	-5.50329	-5.21957	0.7138
C	-7.3761	-4.24674	0.17893

H	-7.59668	-3.98778	1.224
H	-7.90217	-5.18528	-0.03054
C	-7.87969	-3.12969	-0.74305
H	-7.76596	-3.43945	-1.79145
H	-8.94902	-2.95058	-0.5821
C	-7.10284	-1.82742	-0.50618
H	-7.43044	-1.05043	-1.2062
H	-7.29776	-1.45548	0.50693
C	-3.60598	2.46732	4.05368
H	-2.67154	3.01754	3.91559
H	-4.15733	2.93056	4.88019
C	-3.42662	0.96635	4.25427
H	-2.87775	0.7978	5.18707
H	-2.85481	0.51014	3.44008
H	-4.389	0.45428	4.31423
S	4.99542	2.20108	-2.61513
S	3.63856	2.00879	3.50178
S	-0.19714	-4.83706	3.1373
O	6.10933	1.25049	-2.6254
O	5.26162	3.63782	-2.48882
O	5.0461	-1.16355	-1.75553
O	3.87622	-1.17877	2.66685
O	3.53543	3.44854	3.74738
O	4.90644	1.31287	3.74503
O	1.42588	4.29506	2.14569
O	2.44642	4.28045	-2.31951
O	2.63353	-3.46492	-2.37696
O	0.76125	-5.94106	3.02888
O	-1.59272	-5.11129	3.48948

O	2.85363	-4.13077	2.14766
N	4.71432	-1.44966	0.5196
N	1.8461	4.64313	-0.10724
N	3.09959	-3.9007	-0.14738
C	3.97342	1.79603	-1.11413
C	4.18974	0.65618	-0.33013
C	4.73557	-0.71568	-0.67643
C	4.15197	-0.72819	1.57483
C	3.8585	0.64492	1.03322
C	3.32208	1.7599	1.6867
C	2.3132	1.13487	4.38322
H	2.43116	0.08591	4.10012
H	2.61385	1.24696	5.43132
C	0.92021	1.69761	4.12298
H	0.61402	1.54859	3.08241
H	0.87479	2.76723	4.33725
H	0.20129	1.17384	4.76243
C	2.86701	2.78199	0.84569
C	1.98921	3.98697	1.11967
C	2.50451	3.97683	-1.14864
C	3.18045	2.78604	-0.52138
C	1.12344	5.90505	-0.34633
H	0.98031	5.92634	-1.42808
C	1.99293	7.10849	0.07361
H	2.17071	7.06471	1.15632
H	2.96767	7.0223	-0.41937
C	1.31823	8.43595	-0.30181
H	1.25567	8.51156	-1.39645
H	1.94087	9.27265	0.0354

C	5.23028	-2.82042	0.68591
H	4.98207	-3.07911	1.71737
C	4.56812	-3.85618	-0.25819
H	4.7536	-3.55745	-1.2923
C	2.26291	-3.78833	-1.27347
C	0.85654	-4.00031	-0.76416
C	0.92165	-4.06309	0.63604
C	-0.22462	-4.08829	1.43722
C	0.47082	-3.56629	4.24848
H	0.57919	-4.1115	5.19317
H	1.46971	-3.33873	3.86771
C	-0.43627	-2.34882	4.39025
H	-1.44169	-2.63656	4.70488
H	-0.52216	-1.79741	3.4482
H	-0.00783	-1.67436	5.13962
C	2.3789	-4.06746	1.03281
C	5.15852	-5.26022	-0.01071
H	4.8915	-5.5869	1.00207
H	4.69029	-5.96061	-0.71156
C	6.68399	-5.26771	-0.17785
H	6.93926	-5.04373	-1.2231
H	7.06925	-6.27223	0.03194
C	7.34367	-4.23457	0.74349
H	7.18659	-4.52416	1.79207
H	8.42762	-4.21168	0.58234
C	6.76271	-2.834	0.50601
H	7.19911	-2.11202	1.20555
H	7.00906	-2.4946	-0.50734
C	3.92634	1.92101	-4.05537

H	3.08006	2.5989	-3.91662
H	4.53877	2.30238	-4.8807
C	3.53445	0.46153	-4.2593
H	2.9674	0.3753	-5.19248
H	2.90316	0.08975	-3.44615
H	4.41388	-0.18254	-4.32063

Section I. References

1. D. J. Kim, K. R. Hermann, A. Prokofjevs, M. T. Otley, C. Pezzato, M. Owczarek, & J. F. Stoddart, *J. Am. Chem. Soc*. 2017, **139**, 6635−6643.
2. D.-S. Guo, V. D. Uzunova, X. Su, Y. Liu, W. M. Nau, *Chem. Sci.* 2011, **2**, 1722–1734.
3. M. J. Frisch, G. W. Trucks, H. B. Schlegel, G. E. Scuseria, M. A. Robb, J. R. Cheeseman, G. Scalmani, V. Barone, G. A. Petersson, H. Nakatsuji, X. Li, M. Caricato, A. V. Marenich, J. Bloino, B. G. Janesko, R. Gom-perts, B. Mennucci, H. P. Hratchian, J. V. Ortiz, A. F. Izmaylov, J. L. Sonnenberg, D. Williams-Young, F. Ding, F. Lipparini, F. Egidi, J. Goings, B. Peng, A. Petrone, T. Henderson, D. Rana-singhe, V. G. Zakrzewski, J. Gao, N. Rega, G. Zheng, W. Liang, M. Hada, M. Ehara, K. Toyota, R. Fukuda, J. Hasegawa, M. Ishida, T. Nakajima, Y. Honda, O. Kitao, H. Nakai, T. Vreven, K. Throssell, J. A. Montgomery Jr, J. E. Peralta, F. Ogliaro, M. J. Bearpark, J. J. Heyd, E. N. Brothers, K. N. Kudin, V. N. Staroverov, T. A. Keith, R. Kobayashi, J. Normand, K. Raghavachari, A. P. Rendell, J. C. Burant, S. S. Iyengar, J. To-masi, M. Cossi, J. M. Millam, M. Klene, C. Adamo, R. Cammi, J. W. Ochterski, R. L. Martin, K. Morokuma, O. Farkas, J. B. For-esman and D. J. Fox, Gaussian 09, Revision C.01, *Gaussian, Inc., Wallingford CT*, 2016.
4. A. D. Becke, *J. Chem. Phys.* 1993, **98**, 5648−5652.
5. C. Lee, W. Yang and R. G. *Parr, Phys. Rev. B: Condens. Mater.*, 1988, **37**, 785–789.
6. W. J. Hehre, R. Ditchfield and J. A. Pople, *J. Chem. Phys.*, 1972, **56**, 2257–2261.
7. T. Lu, F. Chen, *J. Comput. Chem*. 2012, **33**, 580−592.
8. W. Humphrey, A. Dalke, K. Schulten, *J. Molec. Graphics*. 1996, **14**, 33−38.